Pleistocene and Holocene aeolian facies along the Huelva coast (southern Spain): climatic and neotectonic implications

C. Zazo[1], C.J. Dabrio[2], F. Borja[3], J.L. Goy[4], A.M. Lezine[5], J. Lario[1], M.D. Polo[2], M. Hoyos[1] & J.R. Boersma[6]

[1]*Departamento de Geología, Museo Nacional de Ciencias Naturales–CSIC, c/José Gutiérrez Abascal 2, 28006 Madrid, Spain (e-mail: mcnzc65@mncn.csic.es; lario@mncn.csic.es);* [2]*Departamento de Estratigrafía e Instituto de Geología Económica–CSIC, Facultad de Ciencias Geológicas, Universidad Complutense, 28040 Madrid, Spain (dabrio@eucmax.sim.ucm.es);* [3]*Area de Geografía Física, Facultad de Humanidades, Universidad de Huelva, 21007 Huelva, Spain (fborja@uhu.es);* [4]*Departamento de Geología (Geodinámica), Facultad de Ciencias, Universidad de Salamanca, 37008 Salamanca, Spain (joselgoy@gugu.usal.es);* [5]*Palaeontology and Stratigraphy, URA 1761-CNRS, Jussieu, 75252 Paris Cedex 06, France;* [6] *Department of Physical Geography, Utrecht University, 3508 TC Utrecht, the Netherlands (r.boersma@frw.ruu.nl)*

Received October 1996; accepted in revised form 4 March 1999

Key words: chronology, fluviatile, marine, palynology, sea-level changes

Abstract

The stratigraphic relationships, genesis and chronology, including radiocarbon dating, of the Quaternary sandy deposits forming the El Asperillo cliffs (Huelva) were studied with special emphasis on the influence of neotectonic activity, sea-level changes and climate upon the evolution of the coastal zone. The E-W trending normal fault of Torre del Loro separates two tectonic blocks. The oldest deposits occur in the upthrown block. They are Early to Middle Pleistocene fluviatile deposits, probably Late Pleistocene shallow-marine deposits along an E-W trending shoreline, and Late Pleistocene and Holocene aeolian sands deposited under prevailing southerly winds. Three Pleistocene and Holocene aeolian units accumulated in the downthrown block. Of these, Unit 1, is separated from the overlying Unit 2 by a supersurface that represents the end of the Last Interglacial. Accumulation of Unit 2 took place during the Last Glacial under more arid conditions than Unit 1. The supersurface separating Units 2 and 3 was formed between the Last Glacial maximum at 18 000 ^{14}C yr BP and ca. 14 000 ^{14}C yr BP, the latter age corresponding to an acceleration of the rise of sea level. Unit 3 records wet conditions. The supersurface separating Units 3 and 4 fossilised the fault and the two fault blocks. Units 4 (deposited before the 4th millennium BC), 5 (> 2700 ^{14}C yr BP to 16th century) and 6 (16th century to present) record relatively arid conditions. Prevailing wind directions changed with time from W (Units 2–4) to WSW (Unit 5) and SW (Unit 6).

Introduction

The study area is located in the Neogene basin of the lower Guadalquivir River (southern Spain), where Quaternary morpho-sedimentary units between Mazagón and Matalascañas form the 30-km-long, 20 to 30-m-high El Asperillo littoral cliffs (Figure 1). Most of the rocks along the cliffs consist of weakly cemented white-yellowish sandstone of mainly, but not completely, aeolian origin. A few layers rich in clay and organic matter are interbedded.

Most previous investigations considered the sediments as aeolian and Holocene (Caratini & Viguier 1973). In contrast, Pastor et al. (1976) proposed that most of them are marine and Plio-Pleistocene, and that the only aeolian units, apart from the active dunes, occur in the cliffs above elevations of 15 to 20 m.

Analysis of sedimentary facies along the El Asperillo cliffs allowed Zazo et al. (1981) to interpret the lower and middle deposits of the cliff near Torre del Loro as fluviatile and shallow-marine, respectively.

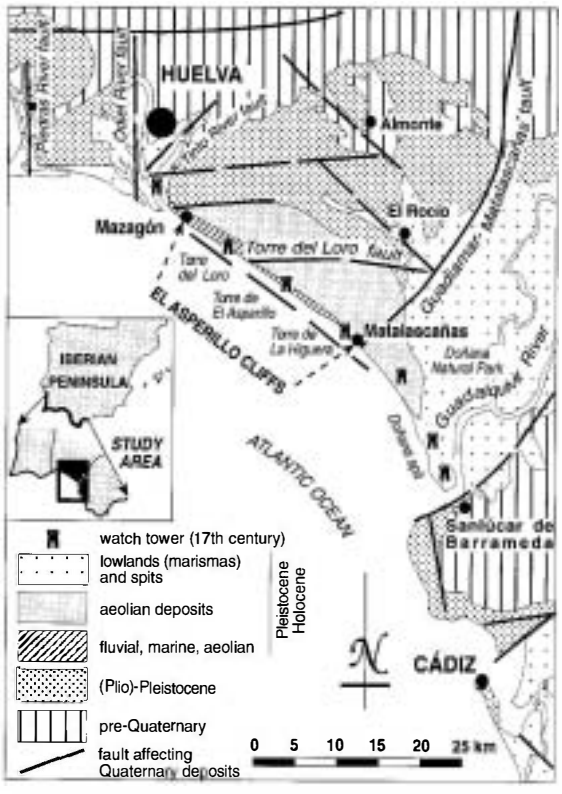

Figure 1. Location map and geological sketch of the El Asperillo area. Note that several river courses follow faults.

Samples collected from a peat layer in the fluviatile sediments at an elevation of 0.5 m yielded an age of 41 000 ^{14}C yr BP (beyond the range of maximum accuracy of the radiocarbon method). The ages of the marine deposits, and of the transition to the overlying aeolian deposits remained unclear.

New dating and mapping of the dune systems, including measurements of palaeowind directions, were incorporated in succeeding papers by Borja (1992) and Borja & Díaz del Olmo (1994, 1996), who correlated the aeolian deposits exposed in the cliff and inland, and who dated the oldest aeolian unit (elevation of sample in the cliff: 16 m) as older than 15 000 ^{14}C yr BP. These and new data led Dabrio et al. (1996) to elaborate preliminary models of aeolian sedimentation.

A neotectonic interpretation, supported by an analysis of the fluviatile drainage pattern, drill cores (IGME 1980), improved radiocarbon dating, and detailed facies analyses, led Goy et al. (1994) to conclude that the E-W trending Torre del Loro fault was active during Quaternary times (Figure 1).

The aim of this paper is to examine the sedimentological features of the rocks exposed along the cliffs, and to interpret the stratigraphic framework of the Early-Middle Pleistocene to Holocene units, and the sedimentary and/or erosional events. We have carried out 28 new ^{14}C radiometric measurements mostly on samples collected in layers rich in organic matter (Table 1). The final goal is to relate these features to neotectonics, sea-level changes and climatic events recognised along the coast of southern Spain.

Sedimentary record of the El Asperillo cliffs

In view of the difficulty of finding landmarks along the El Asperillo cliffs, latitudinal and longitudinal geographical co-ordinates were obtained using a portable Global Positioning System. Distances were measured starting in the ruins of the watch tower of Torre de la Higuera, next to Matalascañas, and continue 25 km to the north-west (Figure 1). Topographic elevations used in the text refer to mean high-water level taken as mean sea level (MSL).

In the uplifted fault block north of the Torre del Loro fault (km 16–25), deposits of three sedimentary environments are recognised from base to top: fluviatile, shallow-marine and aeolian. In the downthrown (south-east) fault block that extends to the resort of Matalascañas (km 16–0), only aeolian sediments occur (Figures 2, 3).

Sediments consist mainly of very well sorted, medium to fine sand. Quartz grains average 80%, plagioclase and potassic feldspars less than 10%. Biotite, tourmaline and other ferro-magnesian minerals are very scarce. Locally, the silt and clay fraction may reach 60% in the topmost part of the fluviatile deposits. Due to the homogeneous mineralogical and petrological composition, the differentiation of units depends on sedimentary structures and other lithological features.

Fluviatile deposits

The lowermost deposits occurring in the upthrown block consist of fine to medium, white to violet sand with conspicuous, reddish, intensely burrowed layers. The maximum observed thickness is <10 m.

Erosional surfaces separate channel-shaped, lenticular bodies, hundreds of metres long and a few metres thick, with width/depth (*w*/*d*, measured perpendicular to the palaeoflow) ratios ranging from 50 to

Table 1. Database of ^{14}C samples and results, El Asperillo cliffs. Sample positions are shown in Figure 3. Elevations expressed in metres above mean sea level (AMSL).

Unit	Sample code	Laboratory-sample code	Sampled material	Elevation (m AMSL)	^{14}C age (yr BP)
Downthrown block					
Unit 5 – Roman – Medieval Dune					
	(6)	LGQ-758	organic sand	18	2590 ± 120[2]
Unit 3					
	MAT-10A	UtC-3937[1]	organic sand	12.8	post 1950
	MAT-10B	UtC-3943[1]	organic sand	12.8	14650 ± 150[2]
	(7)	LGQ-759	peaty sand	12.8	10500 ± 500
	A	LGQ	peaty sand	12.8	6740 ± 220
	B	LGQ	peaty sand	12.8	11240 ± 220
	MAT-18	GX-21838	organic sand	10–12	12690 ± 430
	MAT-17	GX-21837	organic sand	10–12	11480 ± 630
	MAT-13	GX-21833	organic sand	10	13370 ± 660
	Z-2	LGD	organic sand	10	12260 ± 250[5]
Limit Units 2–3					
	MAT-15	GX-21835	organic sand	10–14	24460 +3530/–2450
	MAT-14	GX-21834	organic sand	10–14	18680 ± 910
Unit 2					
	ASP-2	RCD-346	peaty sand	10	22980 ± 400[6]
	a1	LGQ	peaty sand	10	28180 ± 1140
	a2	LGQ	peaty sand	10	20320 ± 400
	a3	LGQ	peaty sand	10	17720 ± 400
	a4	LGQ	peaty sand	10	25320 ± 1390
	b1	LGQ	peaty sand	10	29970 ± 1490
	b3	LGQ	peaty sand	10	28500 ± 1080
	b4	LGQ	peaty sand	10	27130 ± 850
	(4)	LGQ-756	peaty sand	10	29330 ± 1000[3]
	MAT-9	UtC-3934[1]	organic sand	10	28700 ± 700[2]
	MAT-16	GX-21836	organic sand	10–12	40720 +7380/–3780
	MAT-5	UtC-3931[1]	organic sand	10	30700 ± 800[2]
	MAT-4	UtC-3938[1]	wood[4]	4	>45000
Upthrown block					
Unit 5 – Dune					
	MAT-11	UtC-3929[1]	organic sand		2760 ± 60[2]
Fluviatile Unit					
	(3)	LGQ-755	peaty sand	2.5–3	30440 ± 1080[3]
	(2)	LGQ-754	peaty sand	2.5–3	>34170 ± 2590[3]
	MAT-8	UtC-3936[1]	organic sand	2.5–3	43000 ± 5000
	ASP-1	RCD-345	peaty sand	2.5–3	22550 ± 400[6]
	(1)	LGQ-753	peaty sand	2.5–3	>33050 ± 1660[3]
	Z-1	LGD	peaty sand	2.5–3	41000[5]

Key to laboratories: GX: Geochron Laboratories, Massachusetts, USA; LGD: Laboratoire de Géologie Dynamique, Paris, France; LGQ: Laboratoire de Géologie du Quaternaire, Luminy, France; RCD: Radiocarbon Dating, Nottingham, UK; UtC: Van der Graaf Laboratory, Utrecht, Netherlands. Notes: (1) AMS analysis; (2) 'Mean time of residence', beginning of sedimentation must be older that this date; (3) Sample containing some lignite, probably older age; (4) transported piece of *Pinus sp.*; (5) Zazo et al. 1981; (6) Borja 1992.

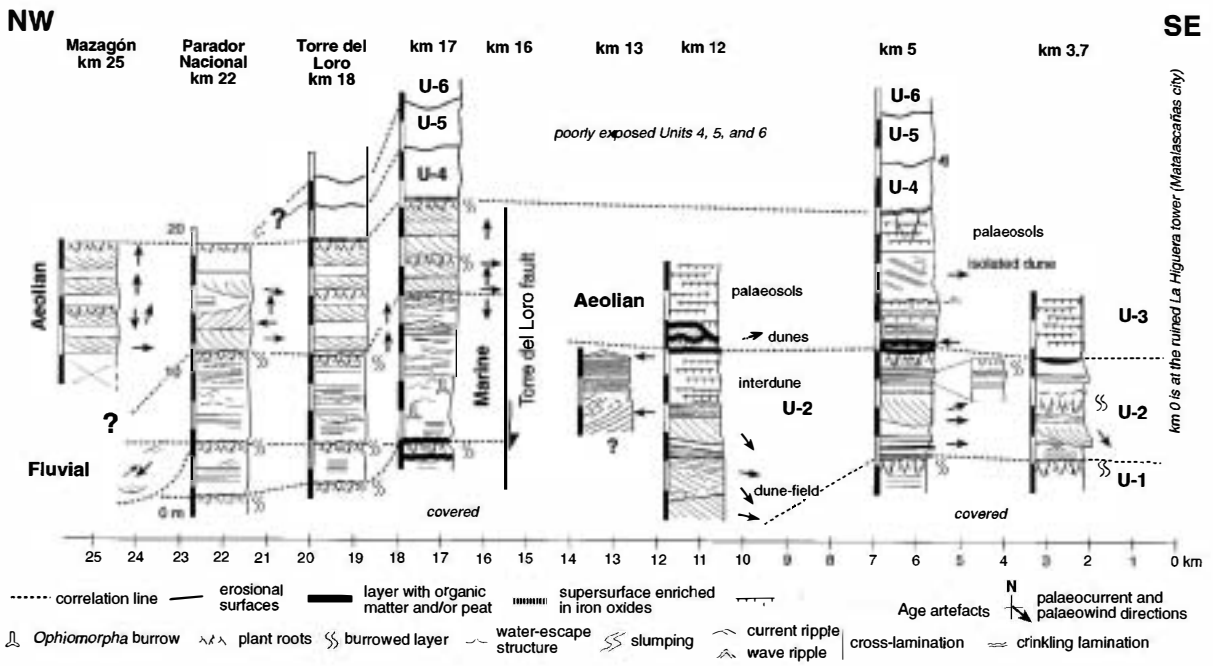

Figure 2. Synthetic stratigraphic sections and correlation in the El Asperillo cliffs. Distances in km from the tower (Torre) of La Higuera. U-1, U-2, etc.: Aeolian Units 1, 2, etc. discussed in text. Palaeocurrent and palaeowind directions shown in map view. ● m at km 22 is the MSL for all sections. Only the visible parts of the sections are shown.

100. The poorly visible internal structure is formed by parallel lamination and trough cross-bedding pointing to the south-west; however, opposite (north-east) directions have been observed near the Parador Nacional de Mazagón (km 22).

These sediments are interpreted as deposited by braided rivers, with tidal influence evidenced by reversing flows. Successive channels are displaced laterally, and typically each channel cuts away the north-western banks of the preceding one, producing an overall displacement towards the north-west of the fluviatile system. The implications of this behaviour will be discussed in a later section.

Moving away from the channels, the erosional surfaces are intensely burrowed and rich in iron oxide that forms vertically elongated concretions of inferred pedogenic origin. Locally, iron concretions coalesce and form continuous crust-like beds. Towards the south-east of Torre del Loro the organic-matter content of the burrowed layers increases and the colour changes to grey (Figure 2). Locally, the upper part is peaty; it was sampled for radiocarbon dating (Figure 3, Table 1). These lateral transitions suggest that channel transport was coeval with pedogenesis.

Regional data (Rodríguez Vidal et al. 1991) and palaeocurrent directions suggest that the fluviatile system was formed by a tributary of the Guadalquivir River during Early to Middle Pleistocene times. Swampy substrata, and reversions of flow indicate that the alluvial plain lay close to the sea.

We interpret the sandy fluviatile deposits (Figures 2, 3) in the upthrown fault block to rest on top of the 70-m-thick, Gravelly Deltaic Unit of Plio-Pleistocene age described by Salvany & Custodio (1995). The top of this lithosome lies 18 m below MSL in Mazagón and 100 m below MSL at Matalascañas.

Radiocarbon measurements in two peaty layers yielded values from 41 000 (sample Z-1), beyond the range of maximum accuracy of the radiocarbon method, to 22 550 ± 400 (sample ASP-1) ^{14}C yr BP, close to the upper (maximum) limit of this range (Figure 3, Table 1).

Marine deposits

Overlying the fluviatile deposits, there is a wedge-shaped body of nonfossiliferous, yellow, fine to medium sands, pointing towards the north-west (Figures 2, 3). The lower limit is an intensely burrowed surface at the top of the fluviatile deposits. Towards the north-

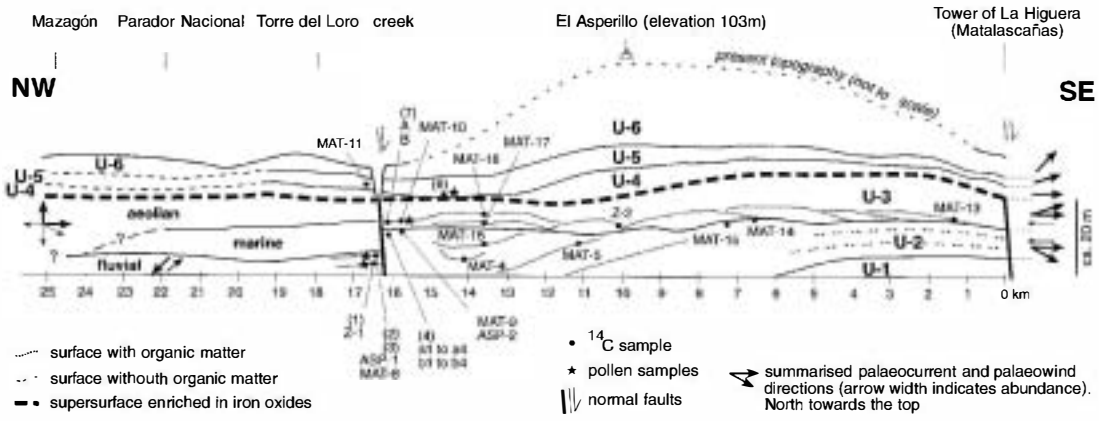

Figure 3. Schematic profile showing distribution of units in the El Asperillo cliffs and sample positions. Distances as in Figure 2. Note strong vertical exaggeration. Palaeocurrent and wind directions shown in map view.

west the internal structure consists of sets of parallel lamination with low-angle truncations. It is similar to that found in recent deposits in the foreshore (Zazo et al. 1981). To the south-east the inconspicuous internal structure consists mostly of parallel lamination that becomes undulating upwards, with isolated sets of low-angle, spoon-shaped cross-bedding. Still further to the south-east, much of the primary sedimentary structure is blurred by widespread dewatering. *Ophiomorpha* burrows, large-scale wave-rippled surfaces, and wave-ripple cross-lamination occur above, and partly also below, the dewatered zone, followed upwards by undulating, hummocky-like cross-bedding and parallel lamination.

According to the facies distribution along the cliffs, we interpret these sediments to be coastal (foreshore) to the north-north-west and shallow marine (shoreface) towards the south-south-east. This implies a coastline trending roughly E-W.

The boundary with the overlying large-scale cross-bedded white sand consists of a conspicuous yellow layer burrowed by plant roots and topped by an erosional surface indicating a noticeable break in sedimentation after deposition of the shallow-marine unit. The limit becomes less distinct towards the north-west.

As no suitable material for radiometric dating was found, and the underlying deposits yielded uncertain results, the age of the marine sediments is difficult to establish. In the absence of conclusive data, we tentatively infer a Middle or Late Pleistocene age.

Aeolian deposits

Aeolian deposits form the upper half of the cliffs in the upthrown block (km 16–25, Figures 2, 3), and the full height of the cliffs visible from the fault (km 16) to the south-east. At first sight, the aeolian deposits seem to be the same on both sides of the fault. However, palaeowind directions argue against this interpretation.

On the upthrown block, between the Torre del Loro and Mazagón, the aeolian deposits consist of very well sorted, white to light-yellow, weakly cemented, medium to fine sand. The most prominent internal structure is formed by large-scale (1.5 to 2 m) tabular cross-bedding with almost perfect parallel lamination in sections normal to palaeowind directions. The major part of avalanche laminae are interpreted as grainflow cross-strata (Hunter 1977, Kocurek & Dott 1981). A closer view reveals that the parallel laminations include cross-lamination, and that a large part of these deposits can be described as the 'subcritical climbing translatent strata' (Hunter 1977, Kocurek & Dott 1981) found in interdune areas.

Many of the planar, neat, interset surfaces are burrowed and some burrows are branching-downwards and interpreted as traces of plant roots. The common reddening provides additional indications of pedogenesis during the development of these surfaces.

Sand textures, set height, and associated burrowing allow us to interpret these rocks as transverse aeolian dunes which migrated towards the north under prevailing southerly winds. Taking into account the preserved thickness of sets, the dune height surpassed 2 m. Predominance of palaeowind directions to the north is a key difference with the aeolian deposits of the downthrown fault block (Figures 2, 3).

The nonfossiliferous nature, the absence of burrowing (apart from the inferred plant roots), lack

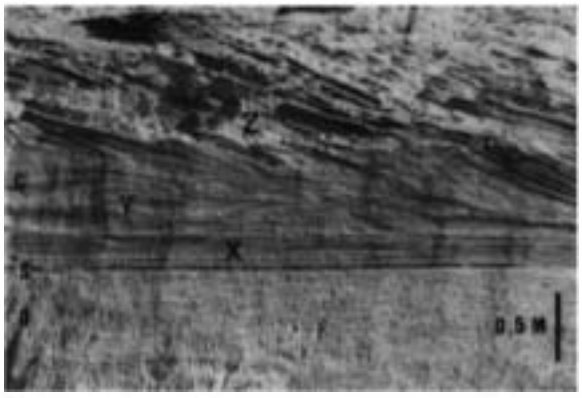

Figure 4. Coset of aeolian cross-strata with a thickening-upwards trend overlying an erosional surface cut into intensely burrowed sands (Unit 2, km 3.75). The section shows a destructive phase (D) and a constructive phase (C) of the dune-field separated by a (major) bounding surface (S) inside Unit 2. The constructive phase consists of low-angle cross-bedded sand sheets (X), thin sets of cross-bedded strata (Y) and thick sets of cross-bedded strata (Z), related to the change from wet to drier substrata with time that allows an increased sand transport.

of wave-ripple cross-lamination, and parallel undulating or hununocky lamination are, further, albeit circumstantial, proofs of a nonaquatic origin.

At least two classes of bounding surfaces (as used by Brookfield 1977, Kocurek 1981, 1988, Kocurek & Dott 1981, Loope 1985, Talbot 1985, Loope & Simpson 1992) can be distinguished: interdune surfaces separate sets of cross-bedding, whereas major surfaces or supersurfaces (Kocurek & Havholm 1993, Havholm & Kocurek 1994) occur associated to vegetation and pedogenesis, and separate discrete sand bodies. Thus, the aeolian sands of the upthrown block represent alternating periods of accumulation and supersurface formation. Most probably, the latter account for the larger part of the time span involved.

On the downthrown block, six units interpreted as aeolian deposits separated by supersurfaces have been distinguished. The three older ones crop out in the cliff wall and their surface equivalents land-inward are uncertain. The three younger units are also observed at the surface, and in the upthrown block. They are clearly distinguished on air photographs (Vanney et al. 1985, Borja 1992, Borja & Díaz del Olmo 1994, 1996). In this paper, these sedimentary units are numbered as Units 1 (bottom) to 6 (top).

'*Unit 1*. Burrowed yellow and red sand'. This unit crops out only in the lower part of the cliffs between km 1 and 6 with a maximum observed thickness of 5 m (Figures 2, 3). It consists of heavily burrowed, yellow to red, fine to medium sand. Blurred parallel-

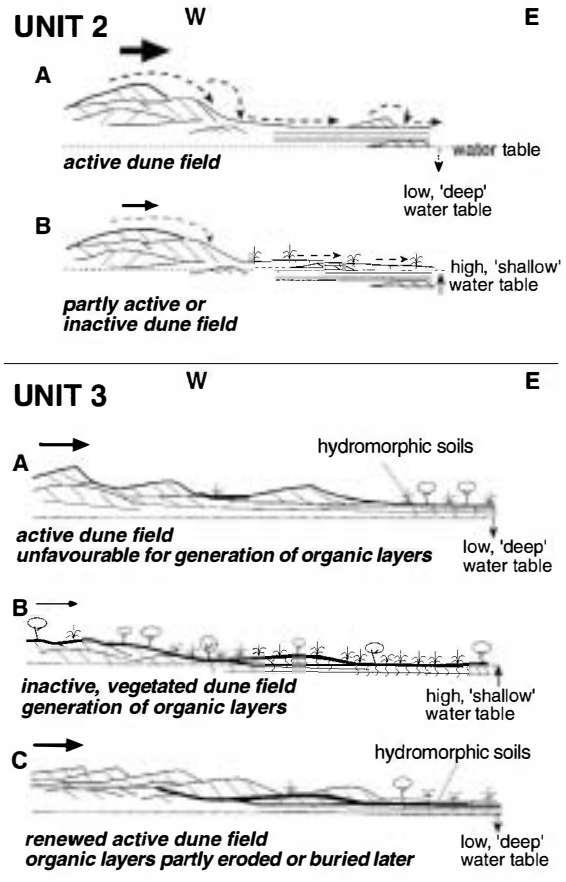

Figure 5. Models for Units 2 and 3 of aeolian and related facies without (A, C) and with (B) significant (but intermittent) plant cover, water-table fluctuations, and pedogenesis (modified from Dabrio et al. 1996).

Figure 6. Interdune facies (Unit 2, km 5). Parallel laminated and crinkling laminated sand (at and below scale bar), ripple cross-lamination (above scale bar), and undulating laminae (top) interpreted as subcritical climbing translatent strata in interdune areas.

lamination has been observed at some localities. Local iron concretions occur.

We interpret these deposits as a vegetated weathering profile under humid conditions that allowed hydromorphism processes and favoured an iron mobilisation and the formation of discoloured vertical zones around plant roots.

In the absence of unequivocal indicators of a sedimentary environment, we interpret this unit to have been deposited in areas where aeolian dune accumulation was impeded by the proximity of the water table to the surface. A likely model for the processes involved are the present lowlands of Doñana (Figure 1).

The thickness of the weathering profile (at least 4 m) and the sharp limit with Unit 2 suggest that this limit represents a remarkable boundary. In fact, it represents a destructive phase of the aeolian system related to stabilisation and erosion, comparable with surfaces described in other settings elsewhere (Talbot 1985, Havholm & Kocurek 1994). These features may be related to a reactivation of the fault that modified the pattern of the deflation and favoured the formation of a super bounding surface or supersurface. Deposition of the overlying Unit 2 took place with much drier substrata and increased supply of sand.

'*Unit 2*. Dune field and interdune deposits'. Unit 2 is the best exposed and most continuous along the cliffs. It consists of very weakly cemented, well-sorted, white and yellow, fine to medium sands. It shows a vertical stacking of aeolian sands, interpreted as dune-field and interdune deposits, which are bounded by laterally continuous surfaces indicative of plant colonisation and dune-field degradation (Figure 3). Two main facies have been distinguished: a) cross-bedded dune facies, and b) laminated interdune facies. These are laterally related.

a) The cross-bedded aeolian dune facies consists of dominantly planar, cross-bedded sands, with sets 1 to 4 m high, and smaller-sized trough cross-bedding, both with predominant palaeowind directions to east and south-east (Figure 4). Avalanche laminae indicate deposition by grain flows and are interpreted as grainflow cross-strata (Hunter 1977, Kocurek & Dott 1981). Locally, the avalanche faces are contorted and brecciated by slumping (Figure 2). These are aeolian dunes (probably transverse or parabolic) migrating under prevailing westerly winds. Dunes accumulated into dune-fields that migrated over interdune areas where thin cross-bedded and parallel-laminated strata occur (Figure 5).

b) The laminated interdune facies consists of horizontal, parallel laminated sands with associated crinkling laminations of the type usually related to adhesion ripples, and of sets of ripple cross-lamination (Figure 6). This facies is similar to the subcritical climbing translatent strata described by Hunter (1977) and Kocurek & Dott (1981), and found in interdune areas. Metre-thick vertical successions with an erosional planar base, a structureless interval, crinkling lamination, and diffuse planar lamination with rootlets, are thought to reflect the rise of the water-table in interdune areas allowing colonisation by grass. As this sequence is repeated vertically, it seems to record oscillations of the water table that are possibly of a periodic (seasonal or longer) character. Isolated sets of cross-bedding interbedded in these deposits, represent dunes detached from the dune fields that migrated into the flatter, depressed interdune areas (Figure 6). The water table probably plays an important role in the deposition and preservation of material in interdune areas, as demonstrated for other areas by Hunter (1977), Loope (1985), Kocurek & Nielson (1986), Loope & Simpson (1992), and Kocurek & Havholm (1993).

There are two types of large-scale bounding surfaces associated to erosional planes in Unit 2. One of these types occurs at the tops of intensely burrowed and reddened horizons (Figure 4). The other occurs at the tops of laterally continuous, decimetre-thick, dark-grey layers of sand, rich in organic matter (Figure 3). In both cases the erosional limits truncate vegetated palaeosoils. The first type occurs in the south-east (km 0–10) whereas the second is found in the north-west (km 10–16).

Both types separate phases of sand accumulation and they can be compared to the stabilised surfaces related to degradation and vegetation, that are in part of erosional origin, and that were described by Talbot (1985). Some of these surfaces can be traced >4 km along the cliffs between km 10 and 16, before they merge into the larger-order bounding surface separating Units 2 and 3 (Figure 3). There are at least four of these units with organic-rich layers in the north-west, but erosion can eliminate the organic layer making it difficult to trace the boundary at certain places.

Repeated evidence of degradation and vegetation of dune-fields suggests a certain periodicity in the supply of sand which we tentatively relate to variations of aridity. However, we lack reliable data to invoke

Figure 7. Interfingering of white cross-bedded sand (formerly active dunes) and dark layers of sand rich in organic matter (inactive, vegetated dunes) that coalesce to form an apparently single, continuous layer of peat. Unit 3, km 8.

a definite orbital forcing (De Boer & Smith 1993, Clemensen et al 1993).

Towards the north-west, in the vicinity (km 13.5–16) of the Torre del Loro fault, a new type of features occurs. This is of younger age than most of the sand bodies bounded by erosional surfaces described above. They consist of irregular erosional surfaces that dip gently towards the north-west, and dissect the aeolian deposits of Unit 2. They form (palaeo)valleys, hundreds of metres wide and several metres deep (*w/d* ranging between 10 and 30, Figure 3). Valley fills consist of a basal layer rich in organic matter including large transported pieces of charred pine logs (sample MAT-4), followed upwards by cross-bedded and parallel laminated sands. The internal structure of aeolian deposits in which the valleys are incised is dominated by cross-bedding. We interpret these buried valleys as generated by runoff during a less arid phase.

'*Unit 3*. Active and fixed dunes and burrowed sands'. These consist of two main facies: a) cross-bedded sands with interbedded layers rich in organic matter, and b) yellow and red sands with burrowed palaeosoil horizons.

a) The cross-bedded sands are similar to those described in Unit 2, but the preserved dunes are smaller (height 1–1.5 m). Dunes are draped by layers rich in organic matter (Figure 7). In some cases, the organic-rich layers decrease in thickness away from the dune troughs, merging up the flanks into erosional surfaces. This facies is interpreted as aeolian dunes moving to the east and north-east, that locally coalesce forming larger accumulations. Vegetation covered and fixed the dunes during phases of reduced dune activity, and plant remains contributed to the development of the layers rich in organic matter, draping the local relief. Repeated fixation and advance of dunes have been recorded in several places as an interfingering of sand and organic layers in cross-bedding (km 8.2–10, Figure 8). As the organic matter is mostly of pedogenic origin, the residence time of carbon makes radiometric dating difficult.

b) The yellow and red, parallel laminated sands with intensely oxidised, burrowed horizons with concretions of iron oxides, are similar to those described in Unit 1. We interpret the burrowed horizons as palaeosoils with a swampy substratum where windblown sands remain trapped. Hydromorphism processes favour the mobilisation of iron and the generation of concretions. White vertical patches correspond to bleached zones around plant roots. The lateral extension of the palaeosoils exceeds 2 km. Red palaeosoils were observed to merge laterally into a dark grey layer of sand with organic matter (e.g. km 5.7). The change takes place <20 m towards the north-west. We interpret facies as the distal end or fringe of a dune, where the wet substratum barred the advanc dunes (Figure 5). Single sets of cross-bedding one or more metres in height and tens

Figure 8. Complex interfingering of sand and peat (arrows) generated during successive reactivations of aeolian dunes and following periods of inactivity and vegetal cover. Dunes wedge out towards the east (at right). Unit 3, km 8.

of metres in length, correspond to aeolian dunes stranded in the wet areas.

These two facies change laterally and vertically (Figure 4): in the lower part of Unit 3 the dune-field facies occurs towards the north-west, whereas the swampy palaeosoil facies predominates towards the south-east. The latter extended rapidly over the whole area. This probably indicates decreasing aridity. Unit 3 records an erosional phase of diminishing aeolian activity related to a widespread humid period, coincidental with the development of a regional supersurface (as defined by Talbot 1985, Kocurek et al. 1991, Havholm & Kocurek 1994). Erosion partially destroyed the topographic irregularities and relief became more uniform. A crust-like horizon of iron oxides accumulated after this erosion, indurating the regional supersurface (Figures 2, 3).

The radiocarbon results of Units 1 to 3 require some consideration (Table 1). Firstly, some of the results from samples of sand rich in organic matter (MAT-5, MAT-9, MAT-10B) express a 'mean time of residence' and thus it is likely that sedimentation began prior to the date obtained. Secondly, some samples of such sands contain lignite and again the true depositional ages must be older than the radiocarbon ages. We assume major lateral movements of these organic interdune deposits, with recycling of material from older layers. Hence, the later dates give a better indication of the dates of deposition.

Unit 1 is of unknown age. Ages obtained for Unit 2 range from older than 30 700 ± 800 to 17 720 ± 400 ^{14}C yr BP (samples MAT-5 and a3 respectively). Radiocarbon data for Unit 3 range between 14 000 and 6 700 ^{14}C yr BP.

'*Unit 4*. Fixed parabolic dunes'. These deposits are well-sorted loose brown cross-bedded sands forming parabolic and locally transverse dunes accumulated in N-S elongated ridges which migrated towards the east. Abundant artefacts of a Late Neolithic to Early Copper industry dated as 4th millennium BC (Díaz del Olmo et al. 1993) occur upon the dunes and post-date the deposition of Unit 4 (Borja 1992).

'*Unit 5*. Partly fixed parabolic dunes'. This unit consists of light-brownish (beige) sands forming large parabolic dunes that migrated towards the east-north-east. Contrary to the underlying units, the dunes preserve some mobility despite the vegetal cover, and they are considered as semi-active.

The age of Unit 5 is post-Early Copper. Radiometric dating of a thin layer rich in organic matter interbedded in the aeolian sands yielded an age of 2760 ± 60 ^{14}C yr BP (sample MAT-11), and a sample of charcoal (sample '(6)') yielded 2590 ± 120 ^{14}C yr BP (Table 1, Figure 3). Locally, the unit contains Roman and Middle-Age archaeological remains (Borja & Díaz del Olmo 1996).

'*Unit 6*. Recent active transverse dunes'. These consist of white sands accumulated in active dunes

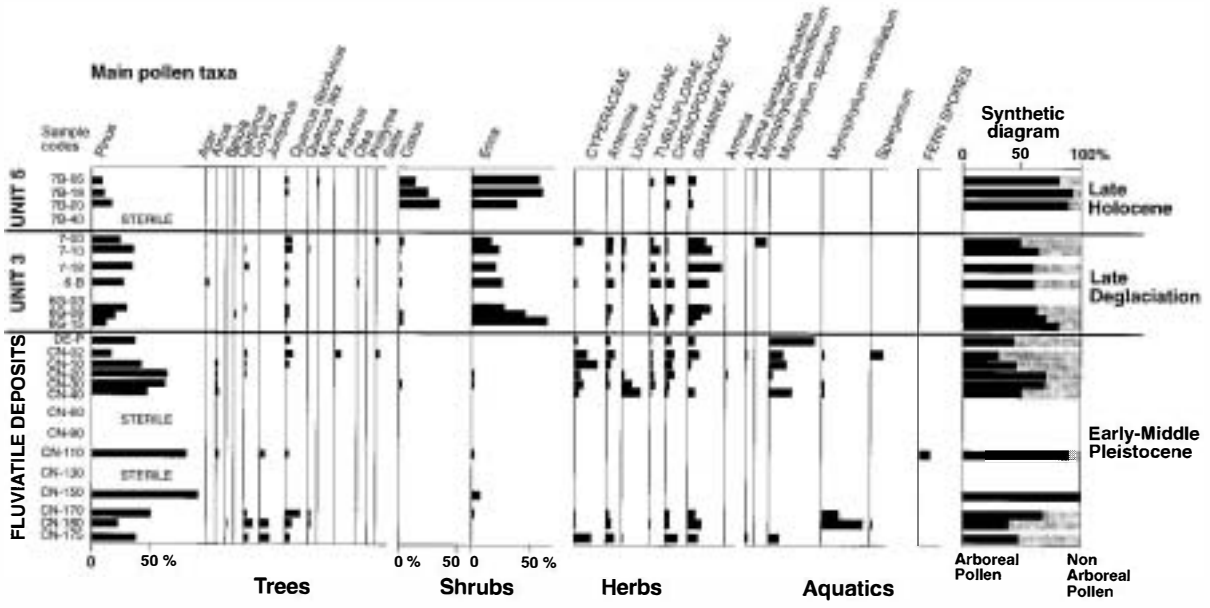

Figure 9. Pollen diagram. Sampled localities are shown in Figure 3.

that coalesce into wide ridges. There is a single ridge in El Asperillo, whereas a dune and slack (interdune) system several kilometres wide occurs in Doñana. The ridges migrate towards the north-east, i.e. they tend to be parallel to the coast (Vanney et al. 1985, Borja 1992, Borja & Díaz del Olmo 1994, 1996).

These dunes contain archaeological remains from the 16th century and onwards, when man-induced deforestation became significant in the area (Borja & Díaz del Olmo 1996).

The coincidence of increased sand supply from the littoral drift (Zazo et al. 1994, Lario et al. 1995) and man-induced deforestation triggered new dunes in some parts of the study area during Unit 6 time, but had little effect where plant cover was preserved.

Pollen analyses of peat layers

Pollen were studied in 24 samples collected from peat layers at the top of the fluviatile deposits and from those interbedded in the aeolian Units 3 and 5 (Figure 3). The samples were processed using the standard HF method (Faegri & Iversen 1975). The 85 determined taxa mainly belong to the modern *'Oleo sylvestris-Quercetum suberis'* thermomediterranean association developed in the area (Rivas Martínez 1987). Their relative frequencies, calculated against the sum of all pollen and spores counted, are presented in Figure 9.

Pollen assemblages allow identification of the local hydrology of the sites and the regional evolution of the vegetation. In relation to the local hydrology, variations of aquatic pollen, especially *Myriophyllum*, allow us to distinguish two groups of samples. This taxon is absent in the samples from the aeolian Units 3 and 5 at locality km 15.5. On the contrary, it dominates the non-arboreal pollen assemblages of the fluviatile deposits at locality km 16.5 (Figure 3). This suggests different hydrological conditions. The *Myriophyllum* appearance is linked to the occurrence of fresh water, the depth of which oscillates between 0.2 to 6 m according to the species. The dominance of *M. spicatum* in the upper part of the peat level (fluviatile deposits) may suggest a water depth of 1 to 6 m, whereas *M. verticillatum* in the lower peat level of the fluviatile deposits suggests a depth of 0.2 to 3 m. Since no main changes in regional vegetation have been recorded in the sites studied, the variations in the hydrology were probably local, and possibly linked to eustatic movements (Lezine & Chateauneuf 1991). The near absence of aquatic plants in the other investigated organic-rich deposits may suggest a lowering of the water table.

With respect to the regional evolution of the vegetation, the assemblages in Units 3 and 5 are mainly composed of shrubs associated with *Pinus*. Ther-

mophilous trees (*Alnus, Betula, Carpinus, Quercus*, etc.) are present with scattered occurrences. The assemblages from Unit 3 are not significantly different from those of Unit 5, except for the presence of Cistaceae and *Artemisia*. The presence of *Artemisia* in Unit 3 might suggest that peat deposition in this unit occurred before the Holocene. As a matter of fact, *Artemisia* practically disappeared from pollen assemblages in El Padul in the province of Granada, 275 km to the east, after 10 000 yr BP (Pons & Reille 1988).

The abundance of *Erica* and *Cistus* in Unit 5 records the degradation of the natural vegetation during the Late Holocene. The abundance of charcoal in the same levels indicates the destruction of the natural vegetation by fire. One cannot observe, however, any indication of other anthropogenic activities such as cultivation of Cerealia or *Olea*.

The absence of *Erica* and *Cistus*, and the occurrence of *Quercus* and *Juniperus* in significant percentages in the samples from the upper part of the fluviatile deposits, suggest that the regional vegetation presented a non-degraded version of the modern thermomediterranean vegetation association described in SW Spain.

It is difficult to place these more or less isolated data into an accurate temporal context. However, comparisons with continuous pollen records from marine and continental sequences located nearby (Lézine & Denèfle in press, Mateus & Queiroz 1991, Van der Knapp & Van Leeuwen 1994, 1995) confirm that they belong to three distinct periods: the Late Holocene (Unit 5), the Last Deglaciation (Unit 3), and, as indicated by the absence of tropical taxa, probably the Early to Middle Pleistocene (fluviatile sequence).

Neotectonic implications

The stratigraphic and geographic arrangement of the sediments exposed along the El Asperillo cliffs indicates neotectonic activity. As outlined in Figure 3, the older fluviatile and marine units suddenly disappear at km 16, where a narrow creek (50 m wide) dissects the present cliff. This stratigraphic anomaly has been interpreted as due to Quaternary normal faulting. The inferred fault would have a similar E-W orientation as the creek, separating a southern downthrown block with Late Pleistocene aeolian units, and a northern upthrown block comprising older, probably Early to Middle Pleistocene, fluviatile, marine and aeolian deposits.

Similar E-W trending normal faults, and conjugated sets of NW-SE faults, have been reported in the whole area from geomorphological analyses (Goy et al. 1994, Flores & Rodríguez Vidal 1994). Nevertheless, the most prominent faulting occurs at NNE-SSW orientations (Figure 1), as is the case of the Tinto, Bajo Guadalquivir and Guadiamar-Matalascañas faults (Viguier 1977, Zazo et al. 1985, 1992, Salvany & Custodio 1995). The latter fault outlines the eastern limit of the coastal segment studied in the present paper. Recently published data, based on extensive hydrological drillings (Salvany & Custodio 1995), indicate a vertical offset close to 150 m for this fault since the Early Pleistocene. The fault is buried at present. Further data from these boreholes indicate a vertical offset of ca. 80 m along the proposed E-W trending Torre del Loro fault for the same span of time. The level used to deduce these values is the top of the Plio-Pleistocene Deltaic Unit in the subsurface of the Guadalquivir basin. It is located 18 to 15 m below MSL in the upthrown block, and 100 m below MSL in the downthrown block (IGME 1980; Salvany & Custodio 1995). At the surface the fault throw is difficult to unravel. The dispersion of radiocarbon ages and the unreliable sedimentological correlation of the aeolian deposits on both sides of the fault make it difficult to calculate the timing and the offset of the fault.

According to subsurface data (Salvany & Custodio 1995) the Torre del Loro fault has been active, at least, since Early Pleistocene times. The migration to the north-west of the channels in the fluviatile Lower-Middle Pleistocene deposits in the upthrown fault block could be due to north-westward tilting of this block.

There is some uncertainty concerning the end of fault activity. At the cliff outcrop the fault is buried by the laterally continuous crust-like layer of iron oxides associated with the erosional supersurface which forms the base of the Holocene Units 4 to 6. The youngest known rocks affected by faulting are the aeolian deposits below this supersurface of the upthrown block (Figure 3), for which we could not find a reliable equivalent in the downthrown block. The submeridian palaeowind directions measured in these deposits do not match the prevailing westerly palaeowinds of the aeolian Units 2 and 3 buried by the same supersurface (Figure 3). This reduces the choices for correlation to Unit 1. If this is the case, then the vertical offset along this fault is probably 18 to 20 m,

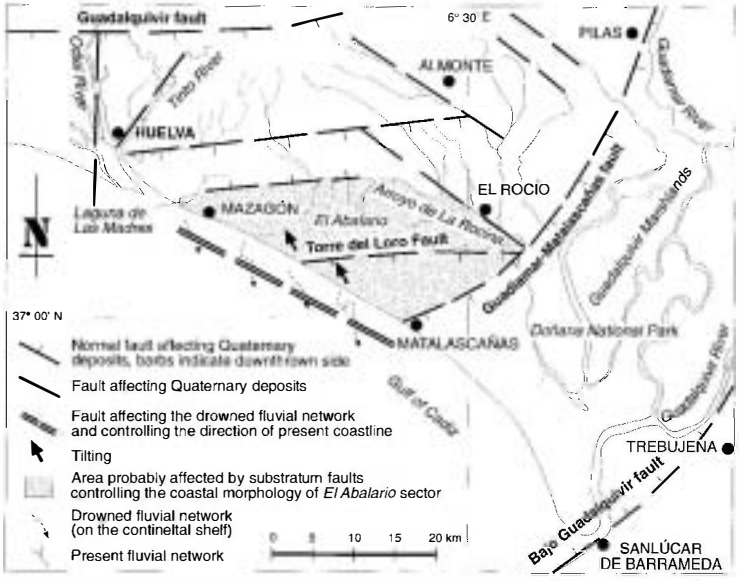

Figure 10. Systems of tectonic structures controlling the coastal morphology and stratigraphy in the El Asperillo area.

and the timing of the last faulting Late Pleistocene, but older than 30 700 ± 800 ^{14}C yr BP, the oldest radiocarbon age yielded by an in situ sample (MAT-5) from Unit 2. This date should be younger if Units 2 and 3 were deposited on the upthrown block and then eroded, but we lack conclusive arguments in this respect. However, there is some evidence of tectonic activity in more recent times. Morpho-sedimentary indicators such as the gentle dip of bounding surfaces towards the north-west and the location close to the Torre del Loro fault of erosional (palaeo)valleys in Unit 2 (Figure 3) suggest synsedimentary tilting of the downthrown block. Slumping structures in cross-bedded strata of Unit 2 might indicate tectonic instability and/or palaeoseismic events.

The normal behaviour deduced for the E-W faults and the major NNE-SSW faults contrasts with the Pleistocene WNW-ESE compressive stress tensor deduced for SW Iberia in recent papers (Ribeiro et al. 1996). This tectonic behaviour has to be ascribed to a complicated interaction between the main Betic foreland faults (NNE-SSW) that control the infilling of the Guadalquivir basin, and subsidiary sets of E-W faults related to the neighbouring major fault that controls this border of the basin, namely the Guadalquivir fault. In this scheme we also include the NW-SE trending normal faults reported by Flores & Rodríguez Vidal (1994) and Goy et al. (1994), which outline individual blocks showing 'domino tectonics' in the Huelva littoral areas. This last set of faults, consistent with the stress tensor orientation mentioned above, represents probably the more recent faults that control the coastal cliff orientation, the strikingly linear drainage patterns, and the drowned palaeo-fluviatile pattern of channels recognised in the Atlantic shelf adjacent to the studied zone (Vanney et al. 1985; Figure 10). The complex fault interactions are a manifestation of the westward expulsion of the Iberian Peninsula during the Eurasian-African collision (Ribeiro et al. 1996). The expulsion is not homogeneous; rather, it takes place along individual crustal blocks promoting major normal faulting in upper crustal levels, as proposed by Goy et al. (1995) for the Gibraltar area. Individual fault-bounded blocks showing differential uplift and subsidence can be defined in the study area, e.g. in the El Abalario sector (Figure 10).

Discussion: climate and sea-level changes

The discontinuous pollen record of the three units sampled at the El Asperillo cliffs does not indicate major climate changes; instead, it suggests vertical oscillations of the water table, which are most probably related to periods of more or less aridity and/or sea-level changes, and not to changes of temperature.

Until now, the only age data available are those for the Las Madres peat bog near Mazagón since 6000

^{14}C yr BP (Zazo et al. 1996a). They show a clear change at 4000 ^{14}C yr BP from a wet period characterised by many Chenopodiaceae to a more arid period dominated by Cyperaceae (*Carex*). A similar, more pronounced change occurs around 1000 ^{14}C yr BP when the peat deposition ceased.

However, some relative climatic changes associated with the deposition of successive aeolian units can be deduced from the sedimentological study. Unit 1 records wet conditions, or a water table close to the surface. Unit 2 records a change to more arid conditions but with wetter episodes indicated by valleys excavated by runoff erosion (Figure 3). Ages obtained for this unit fall into the Last Glacial period. Unit 3 reflects a new increase in humidity and a wet substratum. Most of this unit developed between 14 000 and 10 500 to 11 000 ^{14}C yr BP; a date around 6700 must be considered cautiously because it may correspond to a mean residence time. Dating of the remaining aeolian Units 4 to 6 remains inaccurate, mainly because adequate outcrops are lacking. The only dating of Unit 5 (Table 1) corresponds to a 'mean time of residence' which means that the true age is older. However, the relations of the units with other morpho-sedimentary units in this region (Zazo et al. 1994, Dabrio et al. this issue) and the supersurfaces separating these units can help to refine the climatic interpretation of the recent Holocene.

Archaeological and historical data suggest that the highest rates of deposition measured for Unit 6 correspond to the last 200 years, particularly in the Doñana National Park. During the 17th and 18th centuries most of the natural tree cover (*Juniperus*) was cut and used for firewood in tuna fisheries. The human activity controlled the development of this aeolian unit more than the climatic factor.

The marine deposits in the upthrown block indicate a highstand with MSL close to, or slightly above, the present. This highstand corresponds to an Interglacial that, according to regional data (Zazo & Goy 1989) should be the Last Interglacial (Isotopic Stage 5). This marine episode has not been recognised before along the Huelva coast. It occurs immediately to the south of the Guadalquivir river mouth as two highstands (Isotopic Substages 5e and 5c).

After the deposition of the marine sands, a sea-level drop caused subaerial exposure of a large area which was subject to aeolian deflation. Supply of sand favoured the accumulation of aeolian dune fields. If at least a part of the aeolian deposits in the upthrown fault block are coeval to Unit 1, then they probably represent the end of the Last Interglacial, with a climate, humid enough to favour intense weathering. The supersurface separating Units 1 and 2 represents a temporary cessation of aeolian accumulation.

The development of Unit 2 covers most of the Last Glacial. According to radiometric data, it ended ca. 18 000 ^{14}C yr BP. At that time the Gulf of Cadiz experienced the maximum lowstand of the Glacial Period (Caralp 1992), and MSL was 120 m below its present value (Somoza et al. 1994). Between 18 000 and 13 000 ^{14}C yr BP, sea level rose slowly, as shown in the Portuguese continental shelf (Dias & Boski 1995). During this time the supersurface separating Units 2 and 3 was generated. Unit 3 accumulated under conditions of rapid rise of sea level and wetter conditions than the preceding unit.

The supersurface separating Units 3 and 4 originated around the time when the estuarine barriers reached their most landward position, viz. approximately the time of maximum flooding. From this time (6500 ^{14}C yr BP) onwards, the accumulation of the aeolian Units 4 to 6 appears to be related to the coastal progradation recognised in the spit systems H_1 to H_4 of Zazo et al. (1994) and Dabrio et al. (this issue). Spit progradation took place under more arid conditions and has been interrupted by relatively humid periods lasting 250 to 300 yr during which the regional mean sea-level was slightly higher (Zazo et al. 1996b). Under these conditions the rate at which beach ridges welded to the shore slowed, and particularly wide swales (gaps) were formed. In other places these periods are recorded as erosional surfaces. It is tempting to think that the supersurfaces separating the aeolian Units 4, 5 and 6, and the gaps in progradation might be coeval.

The change of wind direction from west (Unit 4) to WSW and SW (Units 5, 6) may be related to a change to more arid conditions, as indicated in the pollen record of the Las Madres peat bog, at ca. 4000 ^{14}C yr BP (Zazo et al. 1996b).

Conclusions

Normal faults active during the Quaternary conditioned the sedimentation in the coastal zones of SW Spain. The E-W trending Torre del Loro fault was the main control on aeolian sedimentation in the area of the El Asperillo cliffs during the Late Pleistocene, and on the coastline directions during the Middle and Late Pleistocene. Its movement stopped before the

Holocene. Tilting of the upthrown fault block (Torre del Loro and Mazagón) to the north-west during the Early and Middle Pleistocene controlled the displacement towards the north-west of fluviatile channels of a tributary of the palaeo-Guadalquivir River. In this block, marine deposits of probable Last Interglacial age have been preserved, and are subaerially exposed nowadays. Their presence in the area is mentioned for the first time in this paper. In our interpretation, the Torre del Loro fault created accommodation space in the downthrown block where aeolian sediments accumulated during the Last Glacial period, and probably during part of the Last Interglacial. The vertical offset along this fault is 80 m since the Early Pleistocene, and 18 to 20 m during the Late Pleistocene.

At present, the most active normal-fault system trends NW-SE, controlling the direction of the shoreline and the pattern of fluviatile valleys on land and of drowned fluvial valleys on the shelf. This system and the more important NNE-SSW system together separate blocks, like the Abalario sector, in 'domino tectonics' fashion along the Huelva coast.

Six aeolian and aeolian-related sand deposits (Units 1 to 6), stacked in the downthrown block, are separated by bounding surfaces (supersurfaces) in response to major changes in sand supply and wetness of the substratum which controlled the depth of the water table. In contrast, the aeolian deposits below the iron-oxide crust in the upthrown block, thought to correspond to Units 1 to 3, are thinner and deposited on drier substrata. Several supersurfaces marked by palaeosoils indicate repeated degradation and deflation in these deposits.

The generation of the aeolian deposits started prior to the Last Glacial period and continued until the present day. The supersurface separating Units 3 and 4 fossilised the Torre del Loro fault and the two fault blocks. The aeolian Units 4, 5 and 6 accumulated over this new stable area. They are probably related to progradation of spit systems in estuarine barriers. The sedimentation gaps found in the spits may correspond to the supersurfaces separating Units 4, 5 and 6. Both seem to be related to short-lived (250–300 yr), relatively humid periods with a relative rise of sea level.

Wind directions changed during the deposition of the aeolian dunes: the oldest recorded (upthrown fault block) blew towards the north and south. Units 2, 3, and 4 accumulated under prevailing westerly winds. Palaeowinds blew from the WSW during Unit 5 and, as at present, from the south-west during Unit 6. The change in palaeowind directions from Unit 4 to Unit 5 may be related to a change from wetter to more arid conditions since 4000 ^{14}C yr BP, as suggested by the pollen record of the Las Madres peat bog.

Acknowledgements

The work was funded by the Commission of the European Communities, Directorate General for Science, Research and Development (DG XII), Environment Programme, as part of the project 'Climate Change and Coastal Evolution in Europe' (EV5V-CT94-0445). It was also funded by Spanish DGICYT Projects PB95-0109, PB95-0946, and AMB95-1005-CE, UHMA95-001, F. Areces Project 'Cambios climáticos y nivel del mar' (1997–2000), and European Communities Research Fellowship EV5V-CT94-5243. It is a part of the INQUA Shorelines Commission and IGCP Project 437. The authors wish to express their gratitude to N. Combourieu-Nebout for her assistance in pollen analyses and to T. de Groot and the late T.B. Roep who carefully reviewed the manuscript and suggested many improvements.

References

Borja, F. 1992 Cuaternario Reciente, Holoceno y Períodos Históricos del SW de Andalucía. Paleogeografía de medios litorales y fluvio-litorales de los últimos 30.000 años. PhD Thesis, Universidad de Sevilla, 520 pp (unpublished)

Borja, F. & F. Díaz del Olmo 1994 El acantilado de El Asperillo: Cuaternario reciente y fases históricas en el litoral de Huelva – Geogaceta 15: 101–104

Borja, F. & F. Díaz del Olmo 1996 Manto eólico litoral (MEL) del Abalario (Huelva, España): Episodios morfogenéticos posteriores al 22,000 BP. In: Pérez Alberti, A., P. Martini, W. Chesworth & A. Martínez Cortizas (eds) Dinámica y Evolución de Medios Cuaternarios. Xunta de Galicia, Santiago de Compostela: 375–390

Brookfield, M.E. 1977 The origin of bounding surfaces in ancient aeolian sandstones – Sedimentology 24: 303–332

Caralp, M.H. 1992 Paléohydrologie des bassins profonds nord-marocains (Est et Ouest Gibraltar) au Quaternaire terminal: apport des foraminifères bentiques – Bull. Soc. Geol. France 163, 2: 169–178

Caratini, C. & C. Viguier 1973 Etude palynologique et sédimentologique des sables holocènes de la falaise littoral d'El Asperillo (Province de Huelva) – Estudios Geol. 29: 325–328

Clemensen, L.B., I.E.I. Øxnevad & P.L. de Boer 1993 Climatic controls on ancient desert sedimentation: some Palaeozoic and Mesozoic examples from NW Europe and the Western Interior of the USA. In: de Boer, P.L. & D.G. Smith (eds) Orbital Forcing and Cyclic Sequences – Spec. Publs. Int. Ass. Sediment. 19: 439–457

Dabrio, C.J., F. Borja, C. Zazo, R.J. Boersma, J. Lario, J.L. Goy & M.D. Polo 1996 Dunas eólicas y facies asociadas pleistocenas y holocenas en el acantilado del Asperillo (Huelva) – Geogaceta 20: 1089–1092

Dabrio, C.J., C. Zazo, J. Lario, J.L. Goy, F.J. Sierro, F. Borja, J.A. González & J.A. Flores (this issue) Sequence stratigraphy of Holocene incised-valley fill and coastal evolution in the Gulf of Cádiz (Southern Spain)

De Boer, P.L. & D.G. Smith 1993 Orbital Forcing and Cyclic Sequences. In: de Boer, P.L. & D.G. Smith (eds) Orbital Forcing and Cyclic Sequences – Spec. Publs. Int. Ass. Sediment. 19: 1–14

Dias, J.M. & T. Boski 1995 Shoreline evolution in Portugal since the Last Glacial Maximum: a review of current knowledge. In: Ortlieb, L. (ed.) Late Quaternary coastal records of rapid change: Application to present and future conditions, IGCP Project 367, Abstracts Volume 2nd Annual Meeting, Antofagasta, University of Antofagasta: 29–30

Díaz del Olmo, F., Borja, F., Recio, J.M. & Ramos, J. 1993 Evolution paléoclimatologique au Tardiglaciaire et à l'Holocene et presénce de l'homme sur la côte à l'ouest de Cadix (Espagne) – Revue Géomorphol. Dynam. 43: 81–96

Faegri, K & J. Iversen 1975 Texbook of pollen analysis. Munskgaard, Copenhagen, 295 pp

Flores, E. & J. Rodriguez Vidal 1994 Rasgos morfotectónicos del interfluvio costero Guadiana-Guadalquivir (Golfo de Cádiz). In: Amáez, J., J.M. García Ruiz & A. Gómez Villar (eds) Geomorfología en España. Soc. Españ. Geomorfol., Logroño: 13–19

Goy, J.L., C. Zazo, C.J. Dabrio & J. Lario 1994 Fault-controlled shifting shorelines in the Gulf of Cadiz since 20 Ky BP. Abstracts Volume 1st Symposium Atlantic Iberian Continental Margin, Lisboa: 24

Goy, J.L.; C. Zazo, P.G. Silva, J. Lario, T.Bardají & L. Somoza 1995 Evaluación geomofológica del comportamiento neotectónico del Estrecho de Gibraltar (Zona Norte) durante el Cuaternario. Abstracts Volume IV Coloquio Internacional sobre el Enlace Fijo del Estrecho de Gibraltar, Sevilla: 111–122

Havholm, K.G. & Kocurek, G. 1994 Factors controlling aeolian sequence stratigraphy: clues from super bounding surface features in the Middle Jurassic Page Sandstone – Sedimentology 41: 913–934

Hunter, R.E. 1977 Basic types of stratification in small eolian dunes – Sedimentology 24: 361–387

IGME (Instituto Geológico y Minero de España) 1980 Prospección general de lignitos en el Area de Mazagón (Sondeos Asperillo I, II, III, IV, V, VI). Internal report, Empresa Nacional de Investigaciones Mineras Sociedad Anónima (ENADIMSA), Madrid, 25 pp

Kocurek, G. 1981 Significance of interdune deposits and bounding surfaces in aeolian sands – Sedimentology 28: 753–780

Kocurek, G. 1988 First order and superbounding surfaces in eolian sequences – Bounding surfaces revisited – Sediment. Geol. 56: 193–206

Kocurek, G. & R.H. Dott, Jr. 1981 Distinctions and uses of stratification types in the interpretation of eolian sand – J. Sediment. Petrol. 51: 579–595

Kocurek, G. & K.G. Havholm 1993 Eolian sequence stratigraphy – a conceptual framework. In: Weimer, P. & H.W. Posamentier (eds) Recent Advances in and Applications of Siliciclastic Sequence Stratigraphy – Mem. Am. Ass. Petrol. Geol. 58: 393–409

Kocurek, G. & J. Nielson 1986 Conditions favourable for the formation of warm-climate eolian sand sheets – Sedimentology 33: 795–816

Kocurek, G., K.G. Havholm, M. Deynoux & R.C. Blakey 1991 Amalgamated accumulations resulting from climatic and eustatic changes, Akchar Erg, Mauritania – Sedimentology 38: 751–772

Lario, J., C. Zazo, C.J. Dabrio, L. Somoza, J.L. Goy, T. Bardaji & P.G. Silva 1995 Record of recent Holocene sediment input on spit bars and deltas of south Spain. In: Flink, C.W. (ed.) Holocene cycles: Climate, Sea Level and Sedimentation – J. Coastal Res., Spec. Iss. 17: 241–245

Lézine A.M. & J.J. Chateauneuf 1991 Peat in the 'Niayes' of Senegal: depositional environment and Holocene evolution – J. Afr. Earth Sci. 12: 307–310

Lézine A.M. & M. Denèfle (in press) Enhanced anticyclonic circulation in the Eastern North Atlantic during cold intervals of the last deglaciation inferred from deep-sea pollen records – Geology

Loope, D.B. 1985 Episodic deposition and preservation of eolian sands: a late Paleozoic example from south-eastern Utah – Geology 13: 73–76

Loope, D.B. & E.L. Simpson 1992 Significance of thin sets of eolian cross-strata – J. Sediment. Petrol. 62: 849–859

Mateus J.E. & P.F. Queiroz 1991 Holocene palaeoecology of the North-littoral of Alentejo. Field Guidebook International Palaeoecological Excursion 'Holocene Palaeoecology in Portugal, from the South-West Coast to the Serra da Estrela', Universidade de Lisboa, 85 pp

Pastor, F., F. Leyva, F. & C. Zazo 1976 Mapa y Memoria explicativa de la Hoja 1042 (El Abalario) – Mapa Geológico de España, E. 1: 50.000 (2ª Serie) – IGME, Publicaciones del Ministerio de Industria, Madrid, 35 pp

Pons A. & M. Reille 1988 The Holocene- and upper Pleistocene pollen record from Padul (Granada, Spain): a new study – Palaeogeogr., Palaeoclimatol., Palaeoecol. 66: 243–263

Ribeiro, A., J. Cabral, R. Baptista & L. Matias 1996 Stress pattern in Portugal mainland and the adjacent Atlantic region, West Iberia – Tectonics 15: 641–659

Rivas Martinez, S. 1987 Memoria del mapa de las series de vegetación de España escala 1: 400.000. Publ. del Instituto de Conservación de la Naturaleza (ICONA), Madrid, 65 pp

Rodríguez Vidal, J., J.L. Cáceres, J.L. & A. Rodríguez Ramírez 1991 La red fluvial cuaternaria en el piedemonte de Sierra Morena occidental – Cuadernos Investig. Geogr. 17: 37–45

Salvany, J.M. & E. Custodio 1995 Características litológicas de los depósitos plio-cuaternarios del bajo Guadalquivir en el Area de Doñana: implicaciones hidrogeológicas – Revista Soc. Geol. España 8: 21–31

Somoza, L., J.R. Andrés, J. Rey, F.J. Hernandez-Molina, J. Rodriguez Vidal, L. Clemente, A. Rodriguez Ramirez & V. Díaz del Rio 1994 Morpho-depositional evolution of the Cadiz Gulf continental shelf: GOLCA Project. Abstracts Volume 1 Simpósio sobre a margem continental Ibérica Atlântica, Museu Nacional de Historia Natural, Universidade de Lisboa: 55

Talbot, M.R. 1985 Major bounding surfaces in aeolian sandstones – a climatic model – Sedimentology 32: 257–265

Van der Knapp, W.O. & J.F.N. Van Leeuwen 1994 Holocene vegetation, human impact, and climatic change in the Serra Da Estrela, Portugal – Dissertationes Botanicae 234: 497–535

Van der Knapp W.O. & J.F.N. Van Leeuwen 1995 Holocene vegetation succession and degradation as responses to climatic change and human activity in the Serra de Estrela, Portugal – Rev. Palaeobot. Palynol. 89: 153–211

Vanney, J.R., L. Menanteau, C. Zazo & J.L. Goy 1985 MF 02: Punta Umbría-Matalascañas. Mapa fisiográfico del litoral atlántico de Andalucía, E: 1/50.000. Junta de Andalucía, Consejería de Política Territorial, Agencia del Medio Ambiente, Sevilla, 1 map, 28 pp

Viguier, C. 1977 Les grands traits de la tectonique de Basin néogène du Bas Guadalquivir – Bol. Geol. Min. 88: 39–44

Zazo, C. & J.L. Goy 1989 Sea-level changes in the Iberian Peninsula during the last 200,000 years. In: Scott, D.B., P.A. Pirazzoli & C.A. Hoing (eds) Late Quaternary Sea-Level Correlation and Applications. Kluwer Ac. Publ.: 27–39

Zazo, C., C.J. Dabrio, J.L. Goy & L. Menanteau 1981 Parada 'Torre del Loro'. In: Guías de excursiones: 'Estero de Domingo Rubio, Torre del Loro, El Aculadero, Faro de Chipiona'. Actas V^{a} Reunión Grupo Español de Trabajo del Cuaternario, Sevilla: 357–361

Zazo, C., J.L. Goy, C.J. Dabrio, J. Civis & J. Baena 1985 Paleogeografía de la desembocadura del Guadalquivir al comienzo del Cuaternario (provincia de Cádiz, España). Actas I Reunión del Cuaternario Ibérico, Faculdade de Ciencias, Universidade de Lisboa, I: 461–472

Zazo, C., C.J. Dabrio, J.L. Goy & J. Meco 1992 Evolution of the littoral lowlands of Huelva and Cadix (Gulf of Cadix, SW. Spain) from the Flandrian until the Present. In: Suárez de Vivero, J.L. (ed.) The Ocean Change: Management patterns and the Environment. Servicio Publ. Universidad de Sevilla: 27–38

Zazo, C., J.L. Goy, L. Somoza, C.J. Dabrio, G. Belluomini, S. Improta, J. Lario, T. Bardají & P.G. Silva 1994 Holocene sequence of sea-level fluctuations in relation to climatic trends in the Atlantic-Mediterranean linkage coast – J. Coastal Res. 10: 933–945

Zazo, C., A.M. Lézine, F. Borja, M. Denefle, C.J. Dabrio, J. Lario, J. Rodríguez Vidal, J.L. Goy, F. Díaz del Olmo, L. Cáceres, L. Clemente, C. Baeteman, C. & A. Rodríguez 1996a Holocene coastal progradation changes and peat bog development in SW Spanish Coast – INQUA Mediterranean and Black Sea Shorelines Subcommission Newsletter 18: 13–17

Zazo, C., J. Lario, J.L. Goy, T. Bardají, C.J. Dabrio, P.G. Silva & F. Borja 1996b Short periods of relative high sea level since 6,500 ^{14}C yr BP in the Atlantic-Mediterranean region (Iberia). Extended Abstracts 3rd Annual Meeting of IGCP 367 Project, Sydney, Australia: 73–74